The International Journal of Advanced Manufacturing Technology (2018) 96:3881–3891
https://doi.org/10.1007/s00170-018-1836-x

ORIGINAL ARTICLE

Experimental and numerical formability investigation of FML sheets with glass fiber reinforced core

Abdolhossein Jalali Aghchai [1] · Soroush Khatami [1]

Received: 14 May 2017 / Accepted: 25 February 2018 / Published online: 13 March 2018

Abstract
In this study, the formability of the FML (fiber metal laminate) sheets has been investigated by experimental and numerical methods. The sheets consist of an aluminum skin and a glass fiber reinforced core. Uniaxial tensile and stretch forming tests were performed to extract the forming limit diagram (FLD), experimentally. M-K (Marciniak-Kuczynski) method was implemented to extracting the FLD of the FMLs, numerically. The effect of skin and core thicknesses on formability was studied in variable and constant total thickness by numerical method. Finally, it has been cleared that the numerical model predicts the necking strains with less than 9% error. Also, it has been concluded that with doubling of core thickness in constant and variable total thickness, the average formability improves 15 and 23%, respectively, and with tripling core thickness, these values reach to 26 and 53%. In addition, with twofold increase of skin thickness in constant core thickness, the average formability enhances up to 76%.

Keywords FML sheets · Forming limit diagram · M-K method · Finite element method

1 Introduction

Recently, multi-layer sheet metals are used in various industrial areas such as the aerospace, automobile, chemical, and electrical industries. Many of the daily used appliance are made of formed multi-layer sheets. The most important point in forming is to create the desired shape, perfectly. In recent years, many researches have been conducted on forming of the two-layer sheets using the common technologies such as tension, deep drawing, bending, etc. [1]. Wrinkling and severe decreasing of sheet thickness are among main failure modes of forming process. Actually, forming process is defined as the formation of a sheet without occurring failure and tearing of layers. One of the most important criteria in the field of forming process is the formability limits diagrams (FLDs). The FLD concept was first introduced by Keeler and Backofen [2]. Afterwards, Goodwin derived the formability curve of steel in the stamping process [3]. Hecker and Ghosh performed a lot of experimental studies and tried to generate an acceptable accordance between experimental and theoretical results [4]. The FLD of sheet metals represents a relationship between the limits of major and minor principal strains in the plane of the strained sheet, and it depends on the properties such as formability [5]. A forming limit diagram is constructed based on the strain paths obtained from biaxial stretch experiments on different samples and various geometries [6]. The FLDs are obtained through experimental tests, analytical methods, and finally finite element simulations. Owing to interesting mechanical properties such as high bending strength and large mitigation capacity of induced vibration and imposed noise, multi-layer sheets are being used in different industries [7]. On the other hand, forming process of these structures causes some limitations in replacing these materials with conventional one-layer sheets [8].

✉ Abdolhossein Jalali Aghchai
jalali@kntu.ac.ir

Soroush Khatami
skhatami@mail.kntu.ac.ir

[1] Faculty of Mechanical Engineering, K. N. Toosi University of Technology, Tehran, Iran

2 State of the art

Up to now, different aspects of forming of multi-layer sheets are investigated. Kim et al. [5] developed formability evaluation techniques for an automotive part. They adopted formability evaluations (using limit dome height and plane strain test) in order to secure the fundamental data for the

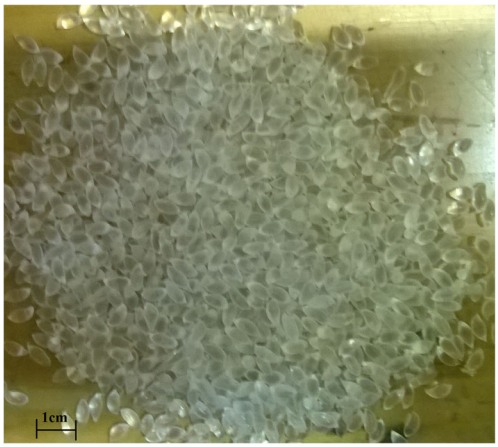

Fig. 1 Polyurethane granola

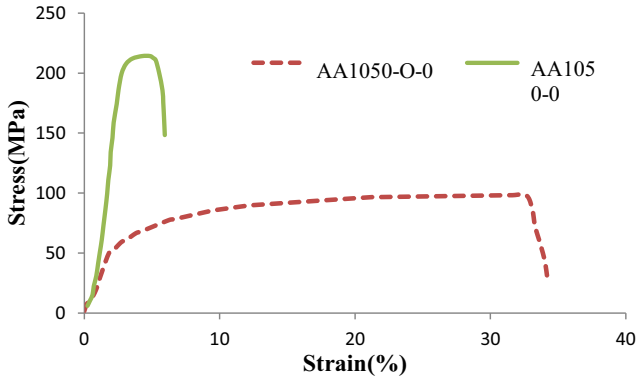

Fig. 3 Engineering stress-strain curve of AA1050 skin sheet before and after heat treatment

measurement of sheet forming and the establishment of optimum forming conditions of the sandwich sheets. One of the analytical approach within this field is the M-K model which was presented by Marciniak and Kuczynski [9]. The M-K model is employed to analyze localized necking in the sheet. Manesh and Taheri [10] studied formability and bond strength of an aluminum-clad steel sheet. Moreover, heat treatment of the sheet was studied, and their results indicated that there is an optimum annealing temperature and time leading to a high bending strength as well as enhanced formability. Gresham et al. [11] investigated the drawing behavior of metal-composite sandwich structure as a function of the constituent material properties and the process variables of blank preheat temperature and blank-holder force. They did find out that blank-holder force has a significant effect on the failure mode of the FML with lower forces resulting in wrinkling as the dominate mode and higher forces resulting in splitting and fracture. Contorno et al. [12] studied the formability of AFS through experiments and finite element analysis. Jalali Aghchai et al. [13] implemented analytical models and an experimental approach to study the formability limits of a two-layer sheet. They realized that the FLD of the two-layer sheet is better than the lower formable component. Parsa et al. [14] incorporated GTN damage model with FEM code so as to predict instability in plastic deformation in sandwich sheet materials with different polymer core thickness ratios. It was observed that the polymer core has both positive and negative effect on FLD of sandwich sheets. The bonding strength of the laminate composites and their mechanism were studied experimentally [15]. It was observed that the bonding strength increased rapidly with the reduction ratio and slightly with the rolling temperature. Sinmazcelik et al. [16] reviewed the background, bonding type, and tests methods of bonding, fatigue, tensile, low and high velocity impact, and blast loading tests for determining the mechanical properties of FMLs. In addition, the effect of surface treatments for better bonding of layers was studied. Sokolova et al. [17] investigated the formability of metal-polymer-metal sandwich composites with embedded different solid and mesh steel inlays with the aim to gain information about their forming behavior by shaping, especially deep drawing and bending. The effects of critical parameters such as rate sensitivity coefficient, stiffness coefficient, and strain hardening exponent on the FLD of two-layer sheet were investigated [18]. It was found that the forming limit of two-layer sheet that lies between the forming limits of its components depends on their material properties. Kalyanasundaram et al. [19] presented results on the stamp forming behavior of the FML systems. Experimental tests were conducted to estimate the major effects of the process parameters that include blank-holder force and temperature. The effect of strain rate and lay-up configuration on tensile and flexural behavior of aluminum-based hybrid fiber metal laminates was studied by Rajkumar et al. [20]. It was observed that tensile strength increased with increasing strain rate; however, the flexural strength decreased with increasing strain

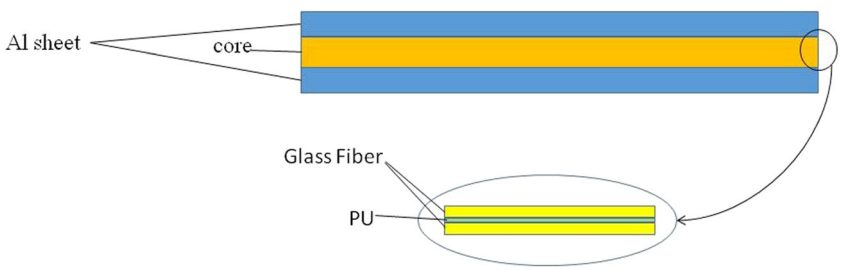

Fig. 2 Cross section of FML sheet

Table 1 Chemical composition of the 1050-O aluminum alloy (mass fraction, %)

Al	Fe	Si	Cu	Mn	Mg	Zn	V	Ti
99.5	0.4	0.25	0.05	0.05	0.05	0.05	0.05	0.03

rate. Prasad et al. [21] investigated the forming limit diagram (FLD) of the Inconel-718 sheet metal experimentally by deforming the material in different strain paths covering from tension-tension to tension-compression mode. Finite element model of the stretch forming process was developed to predict limiting dome height (LDH). It was found that the left side of FLD has higher forming limits compared to right side. Rajabi et al. [22] studied the influence of process parameters and type of core materials on deep-drawing of FMLs through the experimental tests, statistical analyses, and FE simulation. Foteinopoulos et al. [23] proposed an optimization strategy for design and manufacturing of hybrid metal-composite parts. The modeling steps that are essential for the optimization of the production processes were described. Ramzi et al. [24] predicted the forming limit diagram using the 3D simulations of the micro-Marciniak tests with different width, numerically. A conventional Lemaitre ductile damage model with isotropic hardening was used to predict the strain hardening and the necking point. A ductile damage model was used to simulate the stamping operations, and the identification of its parameters was performed by a micro-SPIF test using the finite element updating method. Also, the effect of the initial grain size on the forming limit curves was investigated. Karajibani et al. [25] studied the FLD of the two-layer aluminum-copper sheets by simulation-based approach. In order to construct the FLD, two different criterions including the acceleration (i.e., the second order of derivatives) of equivalent plastic strain and major strain were applied to obtain the onset of necking in the materials.

Despite wide researches on formability of one-layer sheets, both numerically and experimentally, FML sheets have drawn less attention. In this paper, formability of FML sheets with glass fiber reinforced core is studied through experimental analyses. Moreover, a finite element model was developed on the basis of M-K model which then validated by experimental results. FLD diagrams were obtained and compared, and finally, the effects of core and skin thicknesses on the formability of FML sheets were determined.

Table 3 Properties of chopped strand glass fiber

Density (g/cm^3)	E_1 (GPa)	E_2 (MPa)	Nu_{12}
1.5	1.7	3.7	0.27

3 Preparation of FML sheet

A 1050 aluminum alloy sheet with a thickness of 0.5 mm was used as the skin of the FML and PU resin with chopped strand Glass fiber as the core. In order to increase the elongation (at break) of the samples, apply further strains, and decrease the forming force, full annealing heat treatment was done on the aluminum sheet, according to ASM handbook, volume 4. The aluminum samples were put in the dried furnace with the temperature of 345 °C for 30 min. Then, the furnace temperature was lowered to 100 °C in 2 h. Finally, the samples were cooled in the environment temperature. Moreover, for better sticking of the layers, the aluminum sheets were sanded with soft sandpaper, and a washing process, in accordance with standard ASTM D2651, was performed on the sheets. To fabricate the core, grade 65 shore A polyurethane granola (Fig. 1) was placed in the hot press in the 190 °C temperature for 6 min. After making the polyurethane layer, glass fiber was placed in the middle of two polyurethane layer and was pressed in the hot press. The fabricated core was placed between the aluminum skin and pressed in the hot press again. To achieve the desired thickness in each specimen, several steel spacers with corresponding thickness were placed around the specimens in the hot press. Subsequently, FML sheet with the core thickness of 0.2 mm and total thickness of 1.2 was made (Fig. 2).

4 Experimental tests

4.1 Mechanical properties test

Aluminum sheet was cut according to the ASTM E8 M standard. Uniaxial tensile tests were performed on the samples with KOOPA TB-10T machine by rate of 5 mm/min. Figure 3 shows the engineering stress-stain diagram of aluminum before and after heat treatment. Chemical composition and mechanical properties of the aluminum are shown in Tables 1 and 2, respectively. Table 3 shows the properties of

Table 2 Mechanical properties of the 1050-O aluminum alloy

Material	Density (g/cm^3)	Average elongation at break (%)	E (GPa)	Yield strength (MPa)	UTS (MPa)	Poisson ratio
AA1050-O	2.71	35	70.93	35	95	0.33

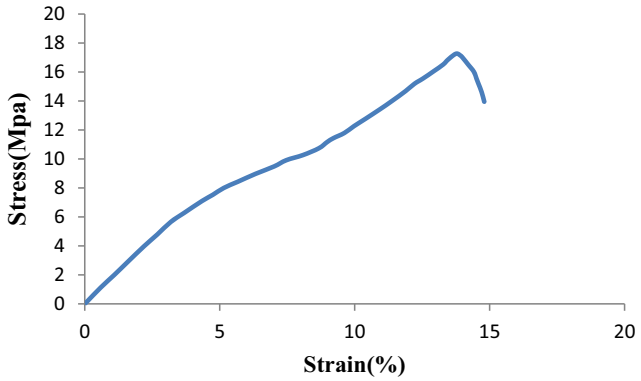

Fig. 4 Engineering stress-strain curve of composite core

chopped strand glass fiber, too. According to the ASTM D638 M standard, the Glass fiber reinforced core of the FML was cut. The test was implemented with Zwick Roell 100. Engineering stress-strain curve of the core is shown in Fig. 4.

4.2 FLD tests

In order to obtain FLD, two types of tests were performed on the samples: uniaxial tensile tests for the left side of the FLD and stretch forming tests for the right side and the plain strain region. Notched strips with various dimensions were used for uniaxial tensile tests, and circular, octagonal, and rectangular samples with different dimensions were used for stretch forming tests. The circle grids were printed on the surface of the samples with waterproof ink and stencil (Fig. 5). The samples were cut with wire cut machine. The dimensions of the samples and the prepared samples are shown in Figs. 6 and 7, respectively.

Stretch forming tests were conducted with hemispherical punch. The die with hemispherical punch and blank holder

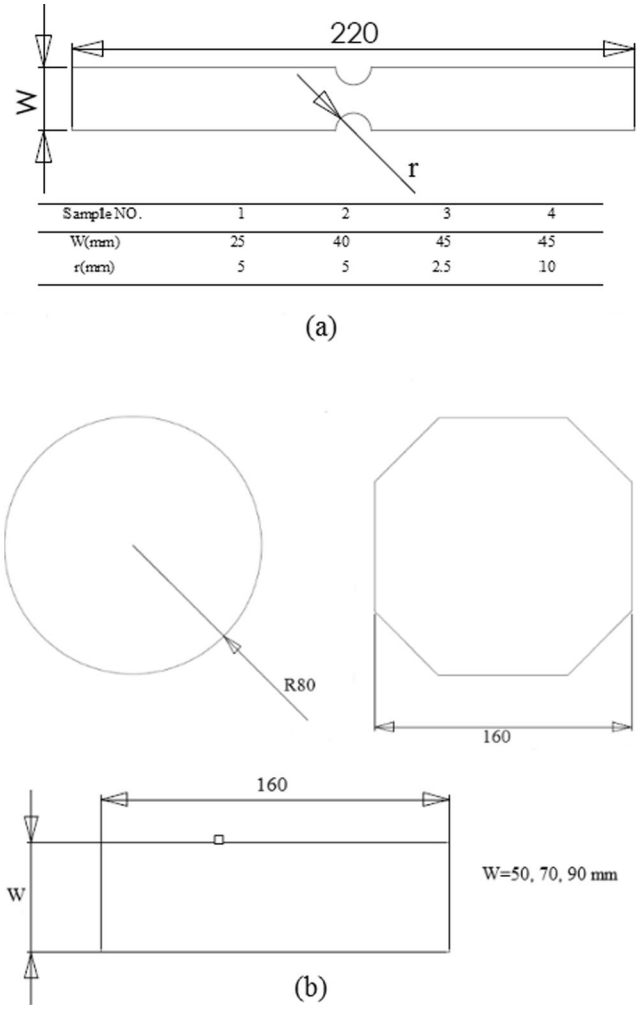

Fig. 6 Dimensions of the test samples. **a** Uniaxial tensile test samples. **b** Stretch forming test samples

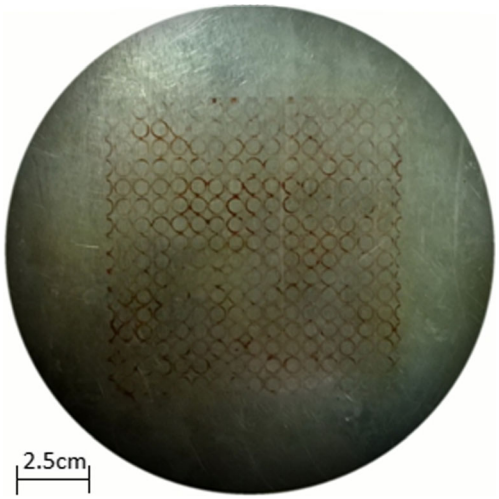

Fig. 5 Sample with printed circular grid

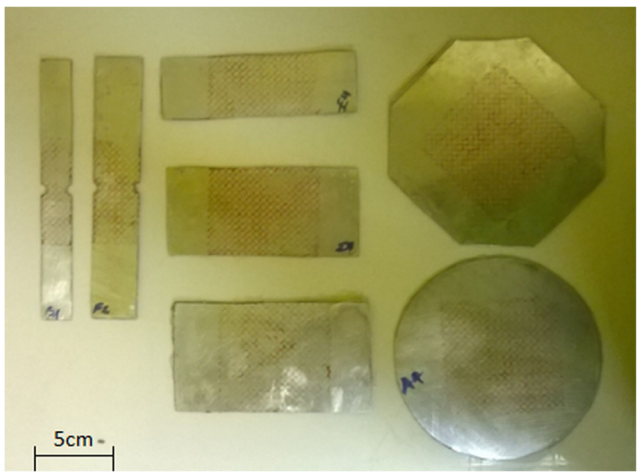

Fig. 7 Prepared samples of FML for experimental FLD tests

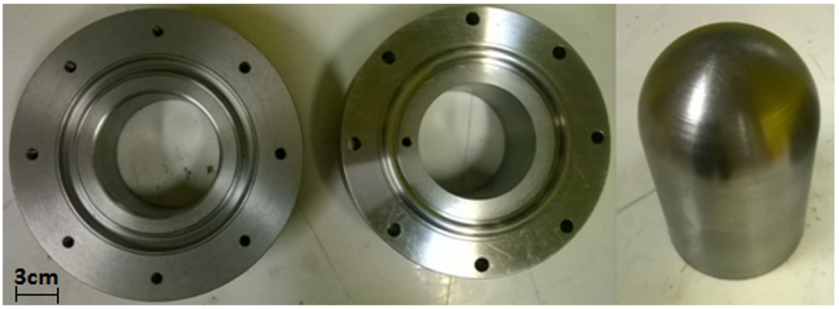

Fig. 8 The matrix, blank holder, hemispherical punch, male bead, and female bead built for stretch forming tests

were made for stretch forming. The diameters of the punch and blank holder were chosen 85 and 85.2 mm, respectively [18]. The matrix, blank holder, hemispherical punch, male bead, and female bead are depicted in Fig. 8. The experiments were conducted with speed of 2 mm/min and 30 kN blank holder force. For determining the appropriate blank holder force, several experiments were done. It has been cleared that in the 30 kN blank holder force, neither wrinkling was occurred nor tearing. When the reaction force of the punch dropped, experiment was stopped. Figures 9 and 10 show the stretch forming test on the circular sample and uniaxial tensile test on the notched strip sample, respectively. After deformation of the samples, the circular grids turn to ellipse. Three nearest ellipses were chosen. With measuring the initial diameter of three circle grid and diameters of those ellipses, the main strains are calculated. An example of these ellipses is shown in Fig. 11.

5 Numerical model

The commercial FE software, Abaqus 6.14, was used to investigate the formability of FML sheet with glass fiber reinforced core. To extract the FLD, two types of modeling were conducted: stretch forming and uniaxial tensile model.

5.1 Stretch forming model

Abaqus/Explicit package was used to model the stretch forming. Stretch forming model was implemented according to the dimensions of die and the samples in Fig. 6b. Because of symmetry in the circular sample, a quarter of the blank was modeled. Since matrix, blank holder, and punch have no deformation and to reduce the computational cost, they had been assumed to be analytically rigid (Fig. 12). The mechanical properties and hardening behavior of aluminum were considered according to Table 2 and Fig. 3. Because there was no sliding and movement between layers in experimental tests, blank layers were modeled as one part. The blank was modeled as one part, and the aluminum was defined as the outer surface of the part. The skin was modeled as isotropic shell material, and the core was modeled as solid material. In the quasi-static analysis, there are two methods for reducing the computational time: first, growing the time increment by increasing the density (mass scaling), and the second,

Fig. 9 Stretch forming test with hemispherical punch

Fig. 10 Uniaxial tensile test on the notched strip sample

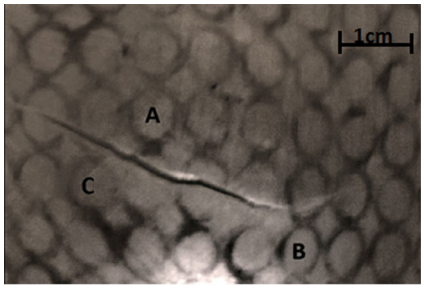

Fig. 11 Three selected ellipses near to the crack

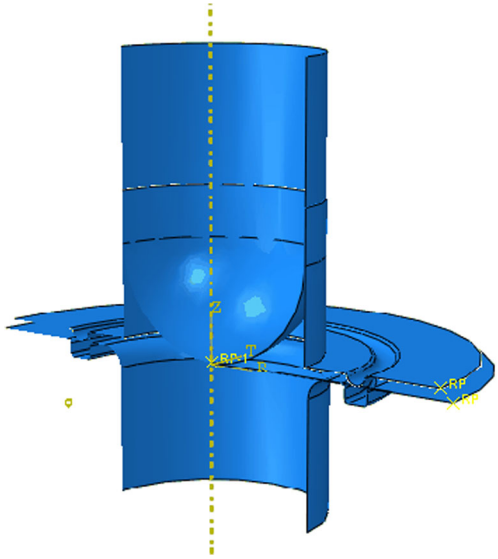

Fig. 12 Cross section of stretch forming finite element model

increasing the loading rate. In this study, the second method was implemented. For finding the suitable step time, the modal analysis was conducted and natural frequency and period were extracted. Natural period was 0.004 s. This time step has been increased and the ratio of kinetic to internal energy controlled. In the quasi-static analysis, this ratio should be under 5% [26]. Eventually, the step time for blank holder loading and punch loading step was chosen 0.06 and 0.08 s. Figure 13 shows the diagram of internal and kinetic energy.

For defining the interaction of parts, tangential behavior and surface-to-surface contact were used. Due to lack of deformation in blank holder, punch and die, the rigid body surfaces were considered as first surfaces, and upper and lower surfaces of the sheet were considered as second surfaces. The friction coefficient of 0.1 was considered between all parts [27–31]. The skin was meshed with S4R, and the core was meshed with C3D8R element. Figure 14 shows the changes of maximum reaction force of the punch and solution time with mesh size. As it can be seen, in the mesh size of 2 mm, the changes of maximum punch reaction force are too low and the solution time is appropriate. Figure 15 shows the meshed blank with four elements in thickness.

For extracting the FLD with M-K method, main strains of a safe element and a failed element was considered. In a period that ratio of growth of main strain in the failed element, to growth of main strain in the safe element, was larger than 7, necking occurred. The strains of safe element in this period were considered as a limit strains. FLD was created by incorporating these limit stain points. Figure 16 shows the strains for safe and failed element. In order to calculate FLD based on punch reaction force, the period that the reaction force of the punch dropped was considered as a necking time, and the strains in the safe element presented as limit strains. For gaining FLD of FML sheet by FLD of aluminum monolayer sheet, the FLD of aluminum monolayer sheet was considered. In the period that FLD criteria in software reached to 1, the element failed and the limit strains constitute the FLD of FML sheet.

5.2 Uniaxial tensile model

In modeling of uniaxial tensile tests, dimension of the sample was considered according to Fig. 6a. In this model, due to lack of contact, Abaqus/standard package was implemented. Step time was selected like the previous case. Properties of FML sheet were defined similar to previous state. One side of the sample was considered as fixed support and displacement

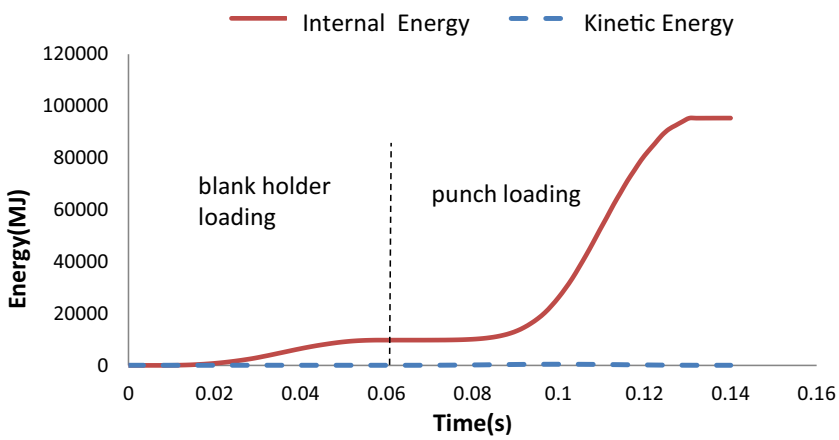

Fig. 13 Internal and kinetic energy curve versus time

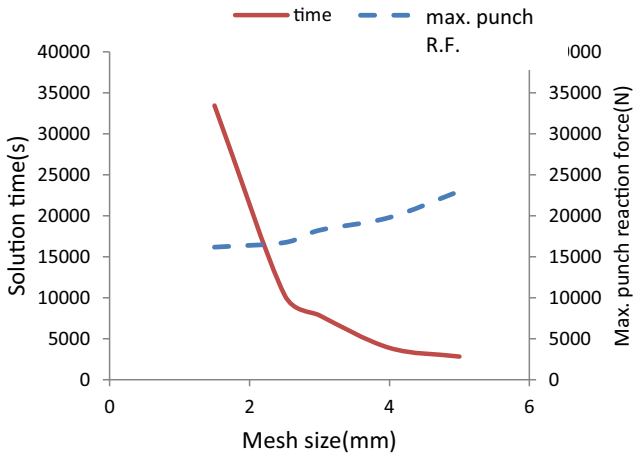

Fig. 14 Changes of max. punch reaction force and solution time versus mesh size

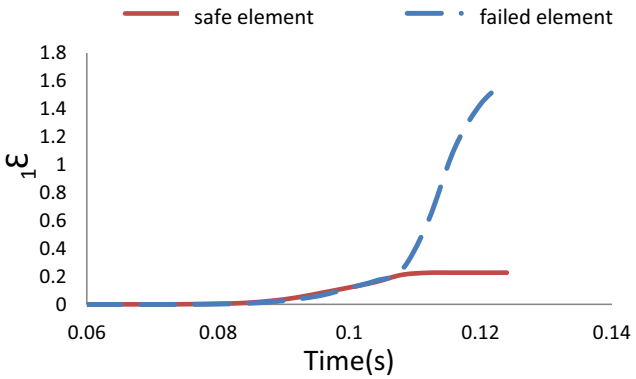

Fig. 16 Main strain of safe and failed element

was applied to the other side support. Calculating and extracting of FLD were performed like stretch forming model. Figure 17 shows the finite element model of uniaxial tensile test sample with 220 × 40 mm dimension and 5 mm notch.

5.3 Models with various core and skin thickness

In order to investigate the effect of core and skin thickness in various and constant total thickness, after validating the numerical model with experimental results, models with different core and skin thickness were considered. Finally, nine types of sheets were created. The thicknesses of core and skin of these sheets are shown in Table 4.

6 Results and discussion

Figure 18 shows the local necking position in the circular sample in the experimental sample and FEM model. Local necking in the experimental sample and FEM model occurred in radius of 22.2 and 21.5 mm, respectively. The values show 4% error. Lack of alignment in the punch and matrix and delay in stopping the punch after drop of reaction force may lead to this error. Positions of tearing in uniaxial tensile test in FEM model and experimental sample are shown in Fig. 19. Experimental and numerical punch force-displacement curves for circular and 70 × 160 mm rectangular sample are shown in Fig. 20. Maximum reaction force differences in experimental and numerical model in circular and 70 × 160 rectangular samples were 3 and 2%, respectively. This amounts in other specimens were 3–8%. In addition, the average error in several selected points along the curve was 3% for all specimens. The reasons of this difference include delay in stopping the punch after drop of reaction force, loss of concentricity in punch and surface of the sample and measurement error in experimental test, and assuming aluminum in the isotropic form in FEM simulation.

Figure 21 shows experimental and numerical FLD of FML sheet with 1.2 mm thickness. For measuring the error, error vectors in several strain paths were calculated. The computed error was 3–9%. Numerical FLD of FML sheet with M-K

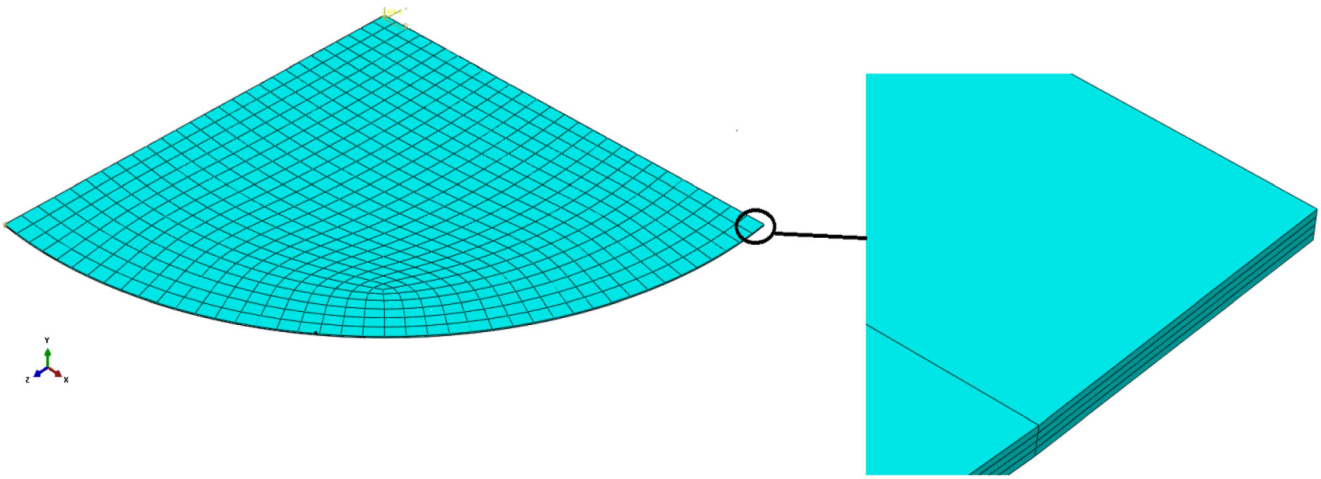

Fig. 15 The meshed blank with 2 mm mesh size

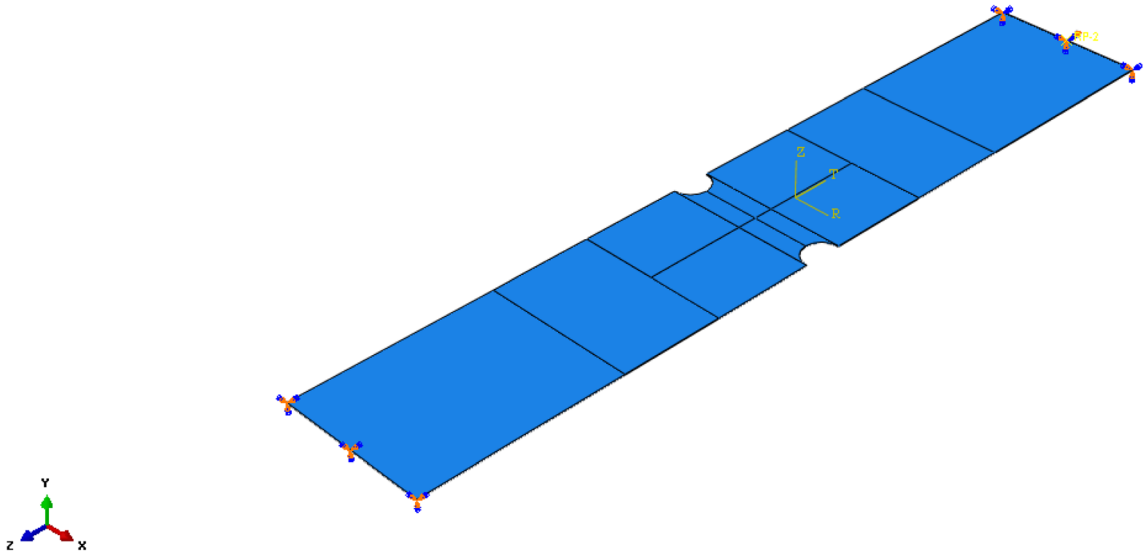

Fig. 17 Finite element model of uniaxial tensile test sample

Table 4 Skin and core thickness of various FML sheets

	FML sheet no.	Core thickness (mm)	Skin thickness (mm)	Total thickness (mm)
Various core thickness and constant skin thickness	1	0.2	0.5	1.2
	2	0.4	0.5	1.4
	3	0.6	0.5	1.6
Various skin thickness and constant core thickness	4	0.2	0.5	1.2
	5	0.2	0.8	1.8
	6	0.2	1	2.2
Increasing of core thickness in constant total thickness	7	0.2	0.5	1.2
	8	0.4	0.4	1.2
	9	0.6	0.3	1.2

theory, FLD criteria of aluminum sheet, and punch reaction force are illustrated in Fig. 22. As we can see, FLD obtained from FLD criteria of aluminum predicts the necking earlier than others. On the negative zone, FLD of reaction force of the punch predicts the necking in larger strains. Errors in comparison to the experimental FLD are 3–9, 1–13, and lower than 11% for M-K theory, FLD criteria of aluminum sheet, and punch reaction force, respectively.

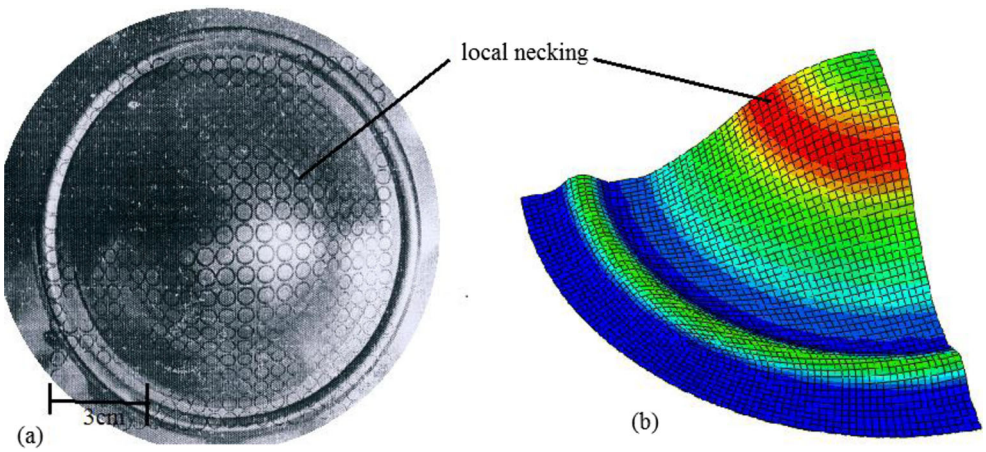

Fig. 18 Local necking position. **a** Experimental sample. **b** FEM model

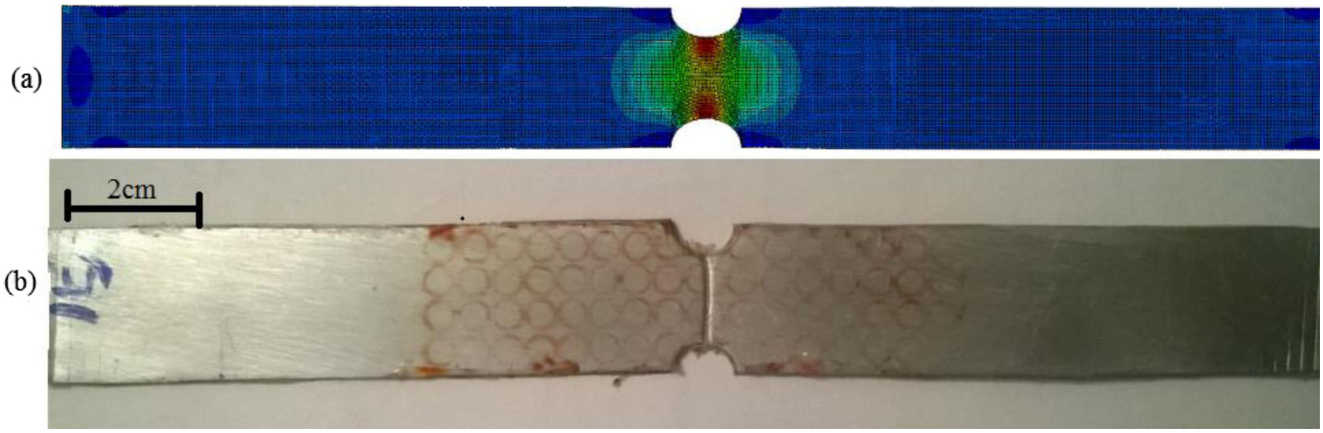

Fig. 19 Position of tearing in uniaxial tensile test. **a** FEM model. **b** Experimental sample

Fig. 20 Experimental and numerical punch force-displacement curve for circular and 70 × 160 mm rectangular sample

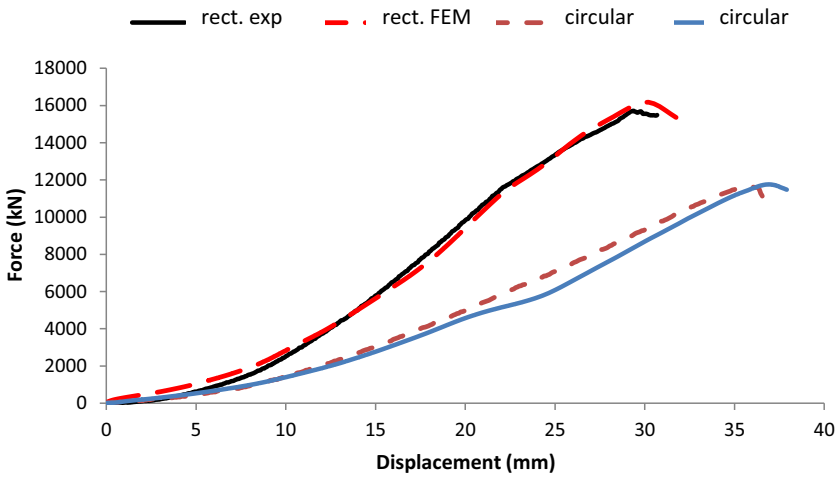

Figure 23 shows FLD of FML sheet with skin thickness of 0.5 mm and core thickness of 0.2, 0.4, and 0.6 mm. With a twofold increase of the core thickness, average formability 23% improves, and with a threefold increase of the core thickness, average formability 53% increases. Increases in core thickness lead to increasing skin distance from the neutral fiber and thereby increasing the flexural stiffness. With increasing the flexural stiffness, stress decreases. If it is

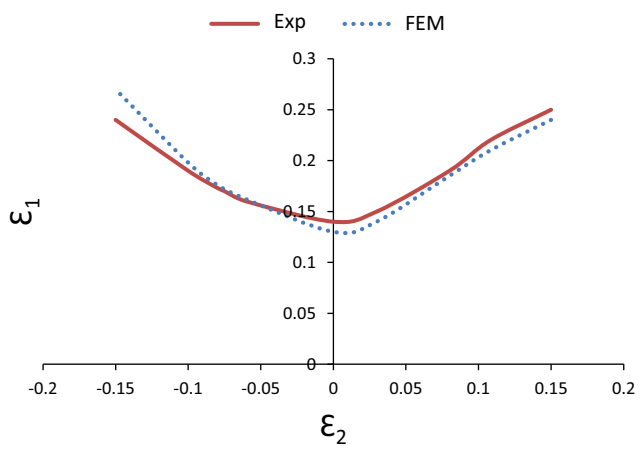

Fig. 21 Experimental and numerical FLD of FML sheet with total thickness of 1.2 mm

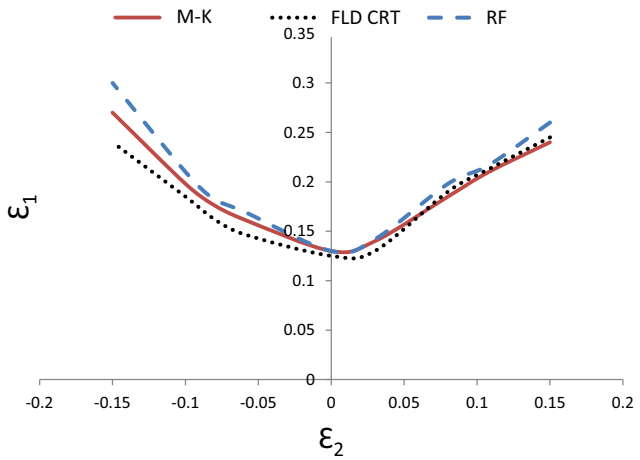

Fig. 22 Numerical FLD of FML sheet with M-K theory, FLD criteria of aluminum sheet, and punch reaction force

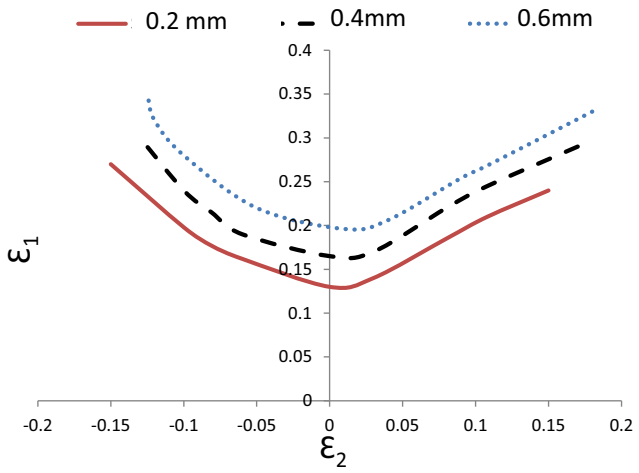

Fig. 23 FLD of FML sheet with skin thickness of 0.5 mm and core thickness of 0.2, 0.4, and 0.6 mm

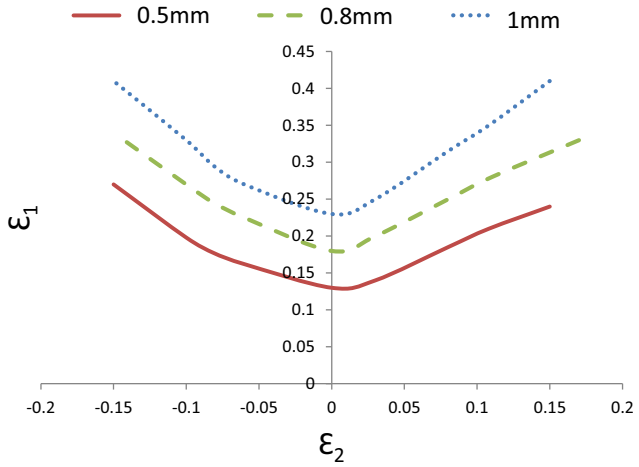

Fig. 24 FLD of FML sheet with core thickness of 0.2 mm and skin thickness of 0.5, 0.8, and 1 mm

assumed that necking occurs in constant tension, when the core thickness increases, the more deformation should be made in the material to attain the necking stress so that with increasing of core thickness in constant skin thickness, the formability has increased.

Also, the maximum reaction forces of the punch for different core thickness are shown in Table 5. With doubling of core thickness, maximum reaction force of punch 6% increases and with tripling of core thickness 11% increases, since total volume of the material increases and required energy for deformation grows. On the other hand, with increases of flexural stiffness, required torque and force for deformation increase.

Figure 24 illustrates the FLD of FML sheet with core thickness of 0.2 mm and skin thickness of 0.5, 0.8, and 1 mm. It became clear that with 60% growth in the thickness of skin, average formability 38% increases and, with doubling of skin thickness, average formability 76% improves. With increasing of skin thickness, flexural stiffness increases and necking stress decreases. Furthermore, formability of skin with growth of its thickness increases. So, it can be concluded that with increasing skin thickness, while the thickness of the core is fixed, FML sheet formability increases.

Figure 25 shows the FLD of FML sheet with constant total thickness of 1.2 mm, skin thickness of 0.5, 0.4, and 0.3 mm, and core thickness of 0.2, 0.4, and 0.6 mm, respectively. As it can be seen, with doubling of core thickness in constant total thickness, average formability 15% improves, and with threefold increase in thickness of core, average formability 26% increases. While with doubling and tripling of core thickness in variable total thickness, average formability 23 and 53% increased, respectively, so that with increasing of core thickness and decreasing of skin thickness in constant total thickness, formability improves.

Table 5 Maximum reaction force of punch in various core thickness

Core thickness (mm)	0.2	0.4	0.6
Max. punch reaction force	16,180	17,167	17,941

7 Conclusions

In this paper, formability of FML sheet was investigated by experimental and numerical methods. FLD of FML sheet with glass fiber reinforced core was presented. Numerical FLD of FML sheet was obtained by M-K theory, FLD criteria of aluminum sheet, and punch reaction force. Effect of core and skin thickness in constant and variable total thickness was studied. All results were concluded in room temperature and could not be generalized to higher temperatures. The following results could be concluded:

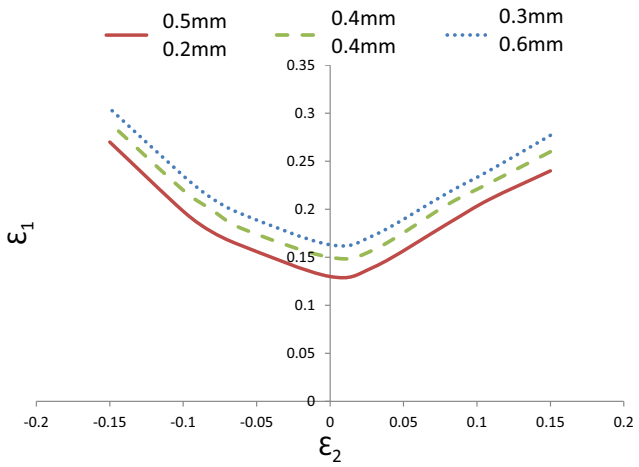

Fig. 25 FLD of FML sheet with constant total thickness of 1.2 mm, skin thickness of 0.5, 0.4, and 0.3 mm, and core thickness of 0.2, 0.4, and 0.6 mm, respectively

- Numerical model of M-K method predicts the limit strains and maximum punch reaction force with 3–9 and 2–8% error, respectively. Also, FLD criteria of aluminum sheet and punch reaction force predict the FLD of FML with 1–13% and under 11% error, respectively.
- FLD criteria of aluminum sheet predict the FLD of FML sheet in smaller strains and cautiously. Punch reaction force predicts the necking in larger strains.
- Average formability of FML sheet with doubling of its core thickness 23% improves and, with tripling of core thickness, 53% increases, while these amounts change to 15 and 26% in constant total thickness of the FML sheet. Also, the maximum punch reaction force increases 6 and 11% with doubling and tripling of core thickness in variable total thickness.
- A 60% increase in skin thickness causes to 38% improvement in average formability of FML sheet with the same core thickness, and with twofold increase in skin thickness, average formability 76% increases.

References

1. Mori T, Kurimoto S (1996) Press-formability of stainless steel and aluminum clad sheet. J Mater Process Technol 56(1):242–253
2. Keeler SP, Backofen WA (1963) Plastic instability and fracture in sheets stretched over rigid punches. Asm Trans Q 56(1):25–48
3. Goodwin GM (1968) Application of strain analysis to sheet metal forming problems in the press shop**.** SAE technical paper
4. Ghosh AK, Hecker SS (1975) Failure in thin sheets stretched over rigid punches. Metall Trans A 6(5):1065–1074
5. Kim KJ, Kim C-W, Choi B-I, Sung CW, Kim HY, Won S-T, Ryu H-Y (2008) Formability of aluminum 5182-polypropylene sandwich sheet for automotive application. J Solid Mech Mater Eng 2(4): 574–581
6. Alcaraz J (1999) Instabilities in bimetallic layers. Int J Plast 15(12): 1341–1358
7. Callister WD (2003) Materials science and engineering an introduction, 6th edn. Wiley
8. Kim K, Kim D, Choi S, Chung K, Shin K, Barlat F, Oh K, Youn J (2003) Formability of AA5182/polypropylene/AA5182 sandwich sheets. J Mater Process Technol 139(1):1–7
9. Marciniak Z, Kuczyński K (1967) Limit strains in the processes of stretch-forming sheet metal. Int J Mech Sci 9(9):609–620
10. Manesh HD, Taheri AK (2003) Bond strength and formability of an aluminum-clad steel sheet. J Alloys Compd 361(1):138–143
11. Gresham J, Cantwell W, Cardew-Hall M, Compston P, Kalyanasundaram S (2006) Drawing behaviour of metal–composite sandwich structures. Compos Struct 75(1):305–312
12. Contorno D, Filice L, Fratini L, Micari F (2006) Forming of aluminum foam sandwich panels: numerical simulations and experimental tests. J Mater Process Technol 177(1):364–367
13. Aghchai AJ, Shakeri M, Mollaei-Dariani B (2008) Theoretical and experimental formability study of two-layer metallic sheet (Al1100/St12). Proc Inst Mech Eng B J Eng Manuf 222(9):1131–1138
14. Parsa M, Ettehad M, Al Ahkami SN (2009) FLD determination of al 3105/polypropylene/Al 3105 sandwich sheet using numerical calculation and experimental investigations. Int J Mater Form 2(1):407–410
15. Zhang X, Tan M, Yang T, Xu X, Wang J (2011) Bonding strength of Al/Mg/Al alloy tri-metallic laminates fabricated by hot rolling. Bull Mater Sci 34(4):805–810
16. Sinmazçelik T, Avcu E, Bora MÖ, Çoban O (2011) A review: fibre metal laminates, background, bonding types and applied test methods. Mater Des 32(7):3671–3685
17. Sokolova OA, Carradò A, Palkowski H (2011) Metal–polymer–metal sandwiches with local metal reinforcements: a study on formability by deep drawing and bending. Compos Struct 94(1):1–7
18. Aghchai AJ, Shakeri M, Dariani BM (2013) Influences of material properties of components on formability of two-layer metallic sheets. Int J Adv Manuf Technol 66(5–8):809–823
19. Kalyanasundaram S, DharMalingam S, Venkatesan S, Sexton A (2013) Effect of process parameters during forming of self reinforced–PP based fiber metal laminate. Compos Struct 97:332–337
20. Rajkumar G, Krishna M, Narasimhamurthy H, Keshavamurthy Y, Nataraj J (2014) Investigation of tensile and bending behavior of aluminum based hybrid fiber metal laminates. Procedia Mater Sci 5: 60–68
21. Prasad KS, Kamal T, Panda S, Kar S, Murty SN, Sharma S (2015) Finite element validation of forming limit diagram of IN-718 sheet metal. Mater Today Proc 2(4–5):2037–2045
22. Rajabi A, Kadkhodayan M, Manoochehri M, Farjadfar R (2015) Deep-drawing of thermoplastic metal-composite structures: experimental investigations, statistical analyses and finite element modeling. J Mater Process Technol 215:159–170
23. Foteinopoulos P, Stavropoulos P, Papacharalampopoulos A, Chryssolouris G (2016) Unified approach in design and manufacturing optimization of hybrid metal-composites parts. Procedia CIRP 55:59–64
24. Ramzi BH, Sebastien T, Fabrice R, Gemala H, Pierrick M (2017) Numerical prediction of the forming limit diagrams of thin sheet metal using SPIF tests. Procedia Eng 183:113–118
25. Karajibani E, Hashemi R, Sedighi M (2017) Forming limit diagram of aluminum-copper two-layer sheets: numerical simulations and experimental verifications. Int J Adv Manuf Technol 90(9–12): 2713–2722
26. ABAQUS analysis user's manual, version 6.14. ABAQUS Inc
27. Liu J, Liu W, Xue W (2013) Forming limit diagram prediction of AA5052/polyethylene/AA5052 sandwich sheets. Mater Des 46: 112–120
28. Zafar R, Lang L, Zhang R (2014) Experimental and numerical evaluation of multilayer sheet forming process parameters for light weight structures using innovative methodology. Int J Mater Form:1–13
29. Hashemi R, Mamusi H, Masoumi A (2014) A simulation-based approach to the determination of forming limit diagrams. Proc Inst Mech Eng B J Eng Manuf:0954405414522448
30. J-g LIU, Wei L, J-x WANG (2012) Influence of interfacial adhesion strength on formability of AA5052/polyethylene/AA5052 sandwich sheet. Trans Nonferrous Metals Soc China 22:s395–s401
31. Morovvati MR, Fatemi A, Sadighi M (2011) Experimental and finite element investigation on wrinkling of circular single layer and two-layer sheet metals in deep drawing process. Int J Adv Manuf Technol 54(1–4):113–121